

Crack effects on the propagation of elastic waves in structural elements

A. Rodríguez-Castellanos, J.E. Rodríguez-Sánchez, J. Núñez-Farfán, and R.E. Olivera-Villaseñor

*Instituto Mexicano del Petróleo,
Eje Central Lázaro Cárdenas 152, D.F. México,
Tel. 9175 6968, e-mail: arcastel@imp.mx*

Recibido el 22 de octubre de 2004; aceptado el 8 de diciembre de 2005

Behavior of the Dynamic Stress Intensity Factor (DSIF) in cracked plates and tubular elements is analyzed. The finite Element Method was used to validate the procedure used by Chen to determine DSIF in a centrally cracked plate loaded with a step function. Once the validation is done, length and orientation of the crack are varied to determine their effect on wave propagation and DSIF values. To expand the study, the analysis is also applied to cracked tubular elements. In all cases, DSIF variation is interpreted as a function of the stresses produced by the interaction of the elastic waves with the boundaries of the structural element studied. Dependence of DSIF values on dilatational, transversal and Rayleigh waves is seen. These elastic waves and their interaction with the structural element boundaries and crack surfaces determine load and unload cycles at the crack tip affecting the stress field and DSIF values.

Keywords: Elastic waves; stress waves; diffraction; dynamic stress intensity factor.

En el presente estudio se analiza el comportamiento del Factor de Intensidad de Esfuerzos Dinámico en placas y elementos tubulares agrietados. Para alcanzar tal objetivo se emplea la técnica numérica conocida como Método del Elemento Finito validando primeramente su aplicación al comparar los resultados con los obtenidos en el problema estudiado por Chen, el cual consiste en cargar dinámicamente una placa centralmente agrietada mediante una función escalón. Una vez realizada la validación, se estudia la influencia de la longitud de la grieta y su orientación y posteriormente se analiza el comportamiento de una sección tubular agrietada. En todos los casos, se evidencia el comportamiento del Factor de Intensidad de Esfuerzos Dinámico, el cual es interpretado como una función de los esfuerzos generados por la interacción de las ondas elásticas con las fronteras del elemento estructural estudiado. Se observa que existe una dependencia completa de tal factor con respecto a las ondas dilatacionales, transversales y de Rayleigh. Por lo tanto, la interacción de las ondas elásticas y las fronteras del elemento estructural determinan ciclos de carga y descarga en la punta de la grieta, afectando el campo de esfuerzos y particularmente la configuración del Factor de Intensidad de Esfuerzos Dinámico.

Descriptores: Ondas elásticas; difracción; factor de intensidad de esfuerzos dinámico.

PACS: 62.20.-x; 62.20.Mk; 62.30.+d

1. Introduction

The presence of cracks in structural elements or mechanical components is, to a certain point, a common case in industrial installations. Such cracks are due to excessive loads, fatigue or even manufacturing and installation defects, which are a cause of reduction in structural integrity. To evaluate the effect of the presence of cracks in structural components, Fracture Mechanics Theory is used; its origins can be referred to Griffith [1]. This is adequate when quasistatic conditions are present and the material shows linear elastic behavior.

In the case of dynamic problems, the inertial characteristic of the problem is very important but its analysis is complicated. One of the first contributions in this area is due to Yoffe [2], who considered that cracks grow by propagating in a perpendicular direction to the maximum main stress. Also, when its speed reaches 60% of the transversal wave speed, cracks change their propagation direction and if such speed increases, the cracks branch out. On the other hand, Craggs [3] investigated semi-infinite cracks (penetrating from the edge far into a body) under dynamic loading conditions and stated that there is a speed limit for crack propagation thus; his conclusions are similar to Yoffe's.

Broberg [4] studied the case of stationary and running cracks loaded by a stress wave for the case of transversal wave propagation. For running cracks, he found that they

grow from an initial length with constant opposite velocities at the two crack tips. His research has had considerable impact in the field of dynamic fracture mechanics in stating that the resistance must be proportional to the crack length in order to comply with the motion. Baker [5] studied the case of a semi-infinite crack in an infinite elastic body subject to a tension load, which propagates at constant speed. This is equivalent to the case of a semi-infinite crack which is being impacted by a stress wave. He showed how stress concentrations behave as a monotonous increasing function, since reflected waves are non-existent. On the other hand, Sih [6] studied the case of a crack under fluctuating stresses and impulse loads. He mentioned that a typical elastic-dynamic analysis can be used for determining the DSIF at the crack tip versus time loading, crack geometry and material parameters. Such information is essential for a better understanding of the response and fracture behavior of dynamically loaded solids. With the same idea, Achenbach y Nuismer [7] assessed the situation of a crack under a stress wave. Their solutions are limited into structures of very large dimensions compared with crack dimensions, thus boundary effects may be neglected in the analysis. Taking in account the effect of the boundaries includes additional analytic difficulties due to the interaction between the crack and the boundaries of the model. Consequently, analytical solutions only exist for selected, relatively simple cases due to this complication.

Freund [8] made a detailed study of Fracture Dynamic problems, proposing solutions to different cases among which the case of cracks under stress waves is considered. He considered that the medium which contains the semi-infinite crack is a homogeneous, isotropic and linear material, under conditions of plane strain. The crack, which is initially stationary, is excited by a stress wave propagating at a constant speed lower than the superficial wave speed. The stress field and the DSIF were obtained by a linear relation.

Numerical methods have been developed for the solution of problems in fracture dynamics such as those related to the interaction of waves in cracked media. Such techniques have been efficient in simulating cracked components under various loads and boundary conditions. Among those numerical methods, the Finite Difference Method has been applied in solving wave propagation problems in cracked media. Chen [9] studied the case of a central cracked plate under an impulsive load using the Finite Difference Method. He found that the stress field in the plate, and particularly at the crack tip, is controlled by the interaction of the stress waves generated by the impulsive load. Variations of the DSIF versus time were found, and it was stated that interaction of elastic waves participate in this variation.

Later, the case of a central cracked plate under an impulsive load was dealt by Frangi [10] using the Boundary Element Method, and by Rodríguez *et al.* [11] using the Finite Element Method. In both cases, the dimensionless DSIF (DSIF divided by the static value) agreed with the results originally obtained by Chen [9,12].

2. Problem definition

Basically, the problem consists in the evaluation of stress waves loading a stationary crack. By “stationary” we mean that crack length is constant and crack tips remain permanently fixed (see Hellan, Ref. 13) in a finite medium. Interaction between three types of elastic waves, the medium boundaries, and crack surfaces are taken into account for determining DSIF variation. In this kind of problem Chen [9]

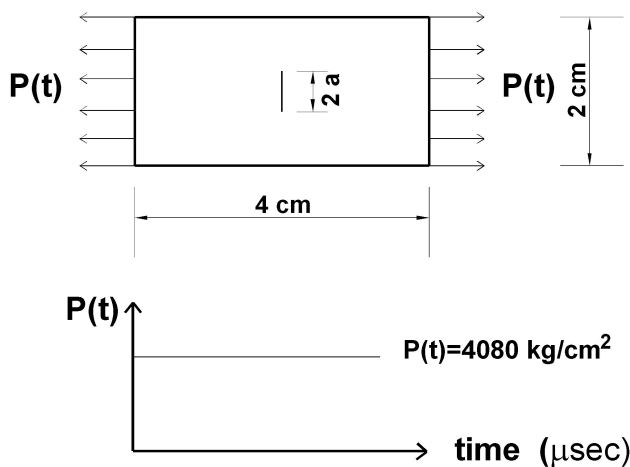


FIGURE 1. Plate with a central crack 0.48 cm in length and step type load pattern analyzed by Chen [9].

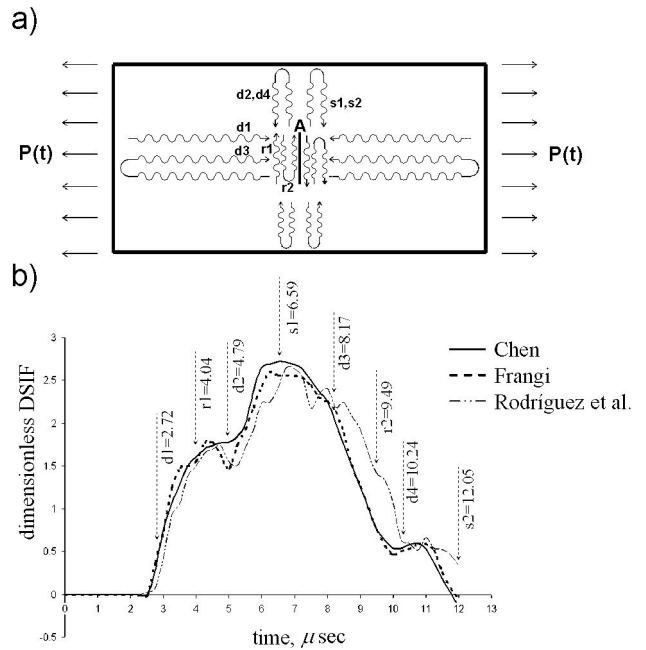


FIGURE 2. a) Simplified representation of an incident wave and diffracted waves in a centrally cracked plate; b) DSIF variation produced by the interaction of diffracted waves in the plate shown in Fig. 1.

was a pioneer and, with Finite Difference Method, analyzed a plate with finite dimensions with a through central crack subject to an axial tension step type load. This is shown in Fig. 1. The mechanical and physical properties of the material are as follows: Elastic module = $1.7 \times 10^6 \text{ Kg/cm}^2$, Poisson ratio = 0.3, and mass density = 5 g/cm^3 . In Fig. 2, Chen’s results are compared with other methods [10, 11]. Excellent agreement is seen. The interaction of elastic waves controls the behavior of the DSIF; this phenomenon is described below.

Figure 2a shows a simplified representation of an impulse load P(t) producing an incident elastic wave defined as d1 which is reflected and diffracted by the crack, generating three types of diffracted waves: Rayleigh (r1), transverse (s1) and dilatational (d2). In addition, d1 is reflected by the face of the crack generating a dilatational wave, defined as d3, which travels towards the edge of the plate and bounces back to the crack tip generating r2, s2 and d4.

The influence of the incident and diffracted waves on the DSIF values at the crack tip is described in Fig. 2b, where it can be seen a complete tension load cycle from time 2.72 to 12 μsec. In this period the DSIF has varied due to wave interactions of diffracted waves by the plate edge and crack faces. Additionally, it can also be seen that up to 2.72 μsec the crack is unloaded, since this is the time taken by the dilatational wave d1 to travel from the edge of the plate to the crack face.

As described before, once the crack face is reached by d1, this wave is diffracted into r1, s1 and d2, and these diffracted waves interact amongst themselves producing a variation of the DSIF at the crack tip (see Fig. 2b). The most influential

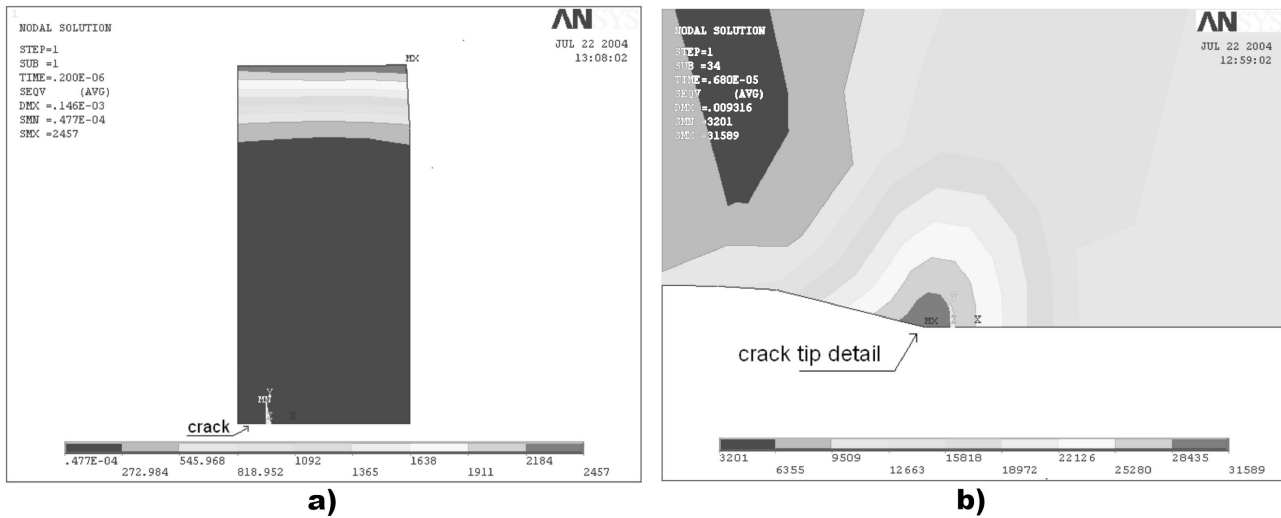


FIGURE 3. Von Mises Stress field: a) for the plate at 0.2 μsec after the load was applied, and b) at the crack tip at 6.59 μsec .

effect on DSIF's from the dilatational waves which initially reach the crack face and are then reflected towards the plate edges where the impulse load was applied, and return compressing the faces of the crack (see d3 in Figs. 2a and 2b). The effect of d3 can be interpreted as a compressive load which forces the crack faces to close, producing a drop in DSIF values from time 8.17 μsec on. In a similar manner to d1, once the crack face is reached by d3, this wave is diffracted into r2, s2, and d4, and their interaction produces a variation of the DSIF as shown in Fig. 2b.

Figure 3a shows a von Mises stress contour at 0.2 μsec , after the impulse load was applied at the top of the figure, and the load travels towards the crack. As mentioned before, it takes 2.72 μsec for the load to reach the crack faces and produce the diffraction phenomenon as previously described. From Fig. 2b, the maximum stress concentration is reached at 6.59 μsec and a stress contour at the crack tip is shown in Fig. 3b. As is known, there is a singularity at the crack tip, which represents a stress field variation of the form $r^{-1/2}$, where r is the radial distance from the crack tip.

Previous results validate the application of ANSYS software for the analysis of DSIF variation at the crack tip under the effect of impulse loads. Further work will show the effect of crack dimensions and crack orientation on DSIF, and the case of DSIF in a tubular section.

3. Transient dynamic analysis

Transient dynamic analysis is a technique used to determine the dynamic response of a structure under time-dependent loads. In this context, when the loads are rapidly applied to the cracked body, the inertial effects must be taken into account, so that the response of the system is measured in a "short-term period of time". In this case of rapid loading, the influence of the loads is transferred to the crack by means of stress waves through the body, see Freund [14]. Therefore, by using this technique, the displacements, strains, stresses and forces can be determined as a time function.

The basic equation of motion solved by a transient dynamic analysis is:

$$[M] \ddot{a}(t) + [C] \dot{a}(t) + [K] a(t) = \bar{F}(t), \quad (1)$$

where, $[M]$ = the mass matrix, $[C]$ = damping matrix, $[K]$ = stiffness matrix, $\ddot{a}(t)$, $\dot{a}(t)$, $a(t)$ are acceleration, velocity, and displacement vectors, respectively, and $\bar{F}(t)$ = load vector. At any given time, these equations can be thought of as a set of static equilibrium equations that also take into account inertia forces. The above equation is solved using the Newmark time integration method for implicit transient analysis, where dynamic displacements $u(t)$ are obtained.

In the Newmark time integration method, the mass, damping, and stiffness matrices are calculated as an initial stage of the analysis. The way in which these matrices are obtained for each finite element is by solving the following equations:

$$M_{ij}^e = \int_{\Omega^e} N_i \rho N_j d\Omega, \quad C_{ij}^e = \int_{\Omega^e} N_i \mu N_j d\Omega$$

and

$$K_{ij}^e = \int_{\Omega^e} B_i^T D B_j d\Omega$$

For a detailed description of these equations see Zienkiewicz [15]. These equations are assembled to represent the complete model and to determine $[M]$, $[C]$, and $[K]$, respectively, which are symmetric. However, determination of $[C]$ is quite difficult due to the lack of knowledge about viscous matrix μ . To avoid this difficulty, Rayleigh damping is used (see Clough and Penzien [16] in which damping matrix is proportional to mass and stiffness matrixes). Figure 4 shows how mass, damping and stiffness matrixes are used in the Newmark time integration method.

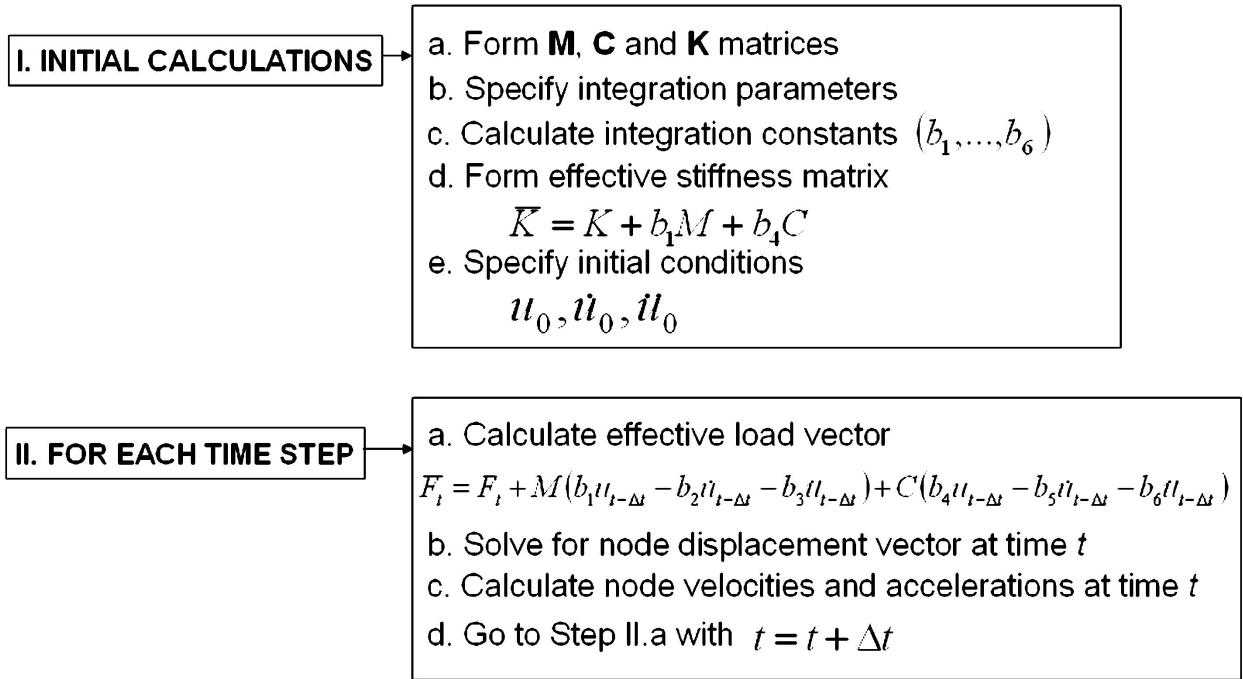


FIGURE 4. Flow diagram of Newmark time integration method applied to transient dynamic analysis.

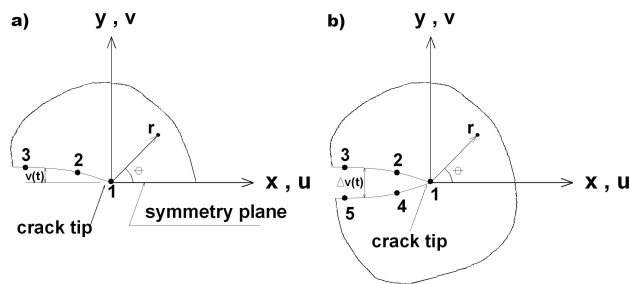


FIGURE 5. Nodes used for the approximate crack-tip displacements: a) half model, and b) full model.

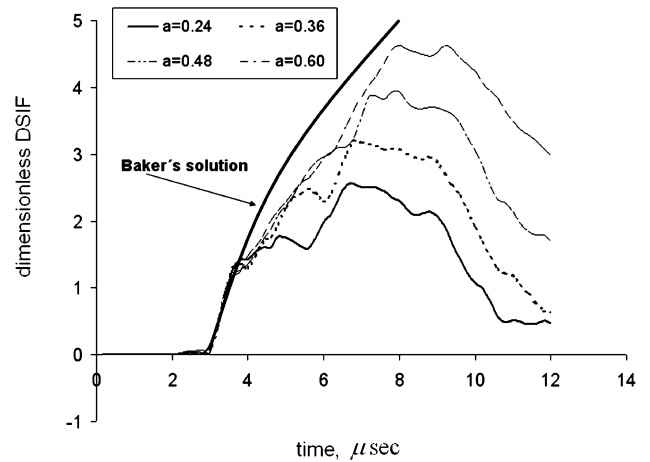


FIGURE 7. Effect of crack size and plate dimensions on DSIF.

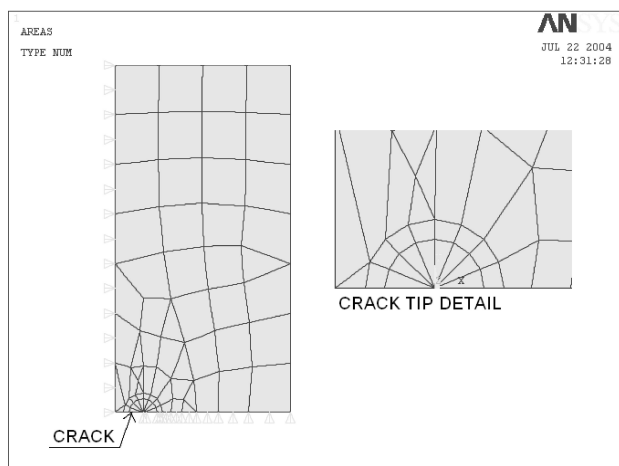


FIGURE 6. Finite Element Model used to analyze a centrally cracked plate (see the fine mesh at the proximity of the crack tip).

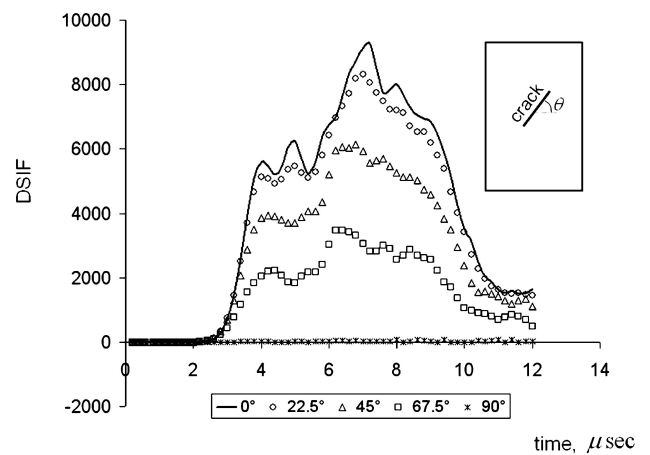


FIGURE 8. DSIF variation for mode I versus crack orientation.

A more complex case of transient analysis application is when no-linear time behaviors are present. In such cases, $[M]$, $[C]$, $[K]$, or $F(t)$ depend on the unknown vector $u(t)$, and therefore these matrices could be updated at each stage.

In dynamic fracture mechanics problems, the most important parameter is the DSIF, which represents the stress singularity of $r^{-1/2}$ near the crack tip; r is the normal distance to the crack tip (see Fig. 5). To evaluate this parameter, the “quarter point element” is often used to model a stress and displacement field near the crack tip. The DSIF is a function of time t , and the way to evaluate it is by knowing the displacements at the crack surfaces in a local coordinate system for half and full models. Expressions used to determine the DSIF such as $K_I^{dyn}(t)$ can be found in [17].

4. Analysis of a centrally cracked plate

Figure 6 shows a fourth of the meshed model used (due to symmetry simplifications) for the analysis of a centrally cracked plate to determine DSIF using the Finite Element Method incorporated in the ANSYS ver. 6 software. The mesh has 62 elements, eight of which are located at the crack tip, with their central nodes displaced one-fourth of the element dimension in order to simulate the singularity that represents the crack tip, making it possible to determine the DSIF. Since only one-fourth of the entire plate was modeled, appropriate boundary conditions were determined to provide continuity and symmetry for displacements and tractions, horizontally and vertically.

Figure 7 shows DSIF values by increasing the crack size on the previously described model. Material properties and plate dimensions are the same as described in Sec. 2 and Fig. 1, respectively, which represent the model used by Chen. In this case, crack size was varied taking the following values: $a = 0.24, 0.36, 0.48,$ and 0.60 cm. In general terms, the DSIF plot in Figure 7 shows a similar pattern to that shown in Fig. 2. By increasing the crack size, the DSIF is strongly

influenced by dilatational waves; this assumption is based on the fact that, for longer cracks, Rayleigh and transversal waves produced by crack diffraction take longer to interact with the crack tips. Consequently, before interaction takes place, the growth rate of the DSIF curves is similar to Baker’s

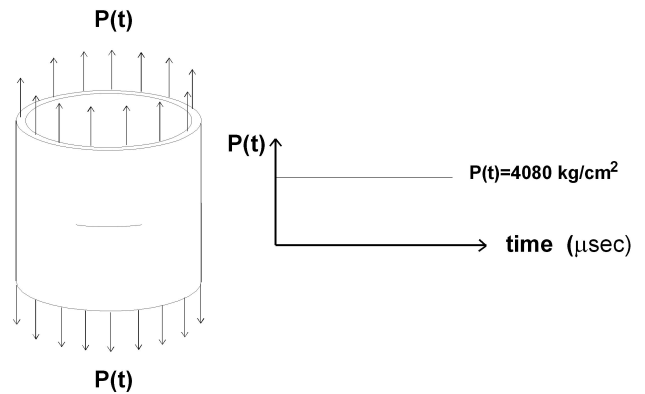


FIGURE 9. Cracked tubular section and step tension load applied.

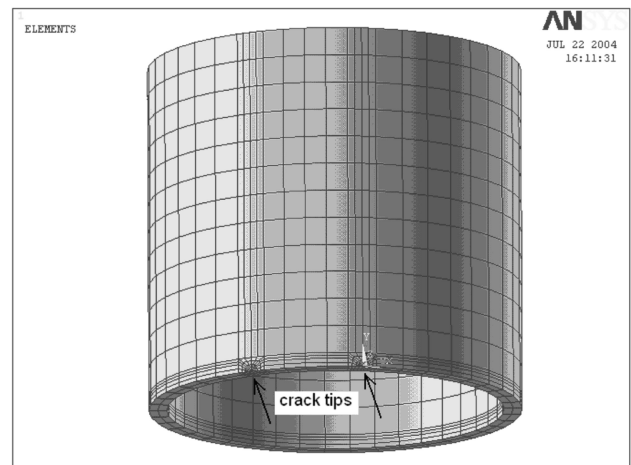
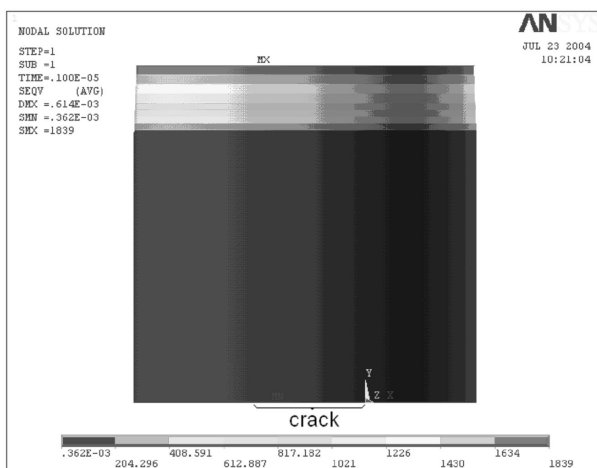
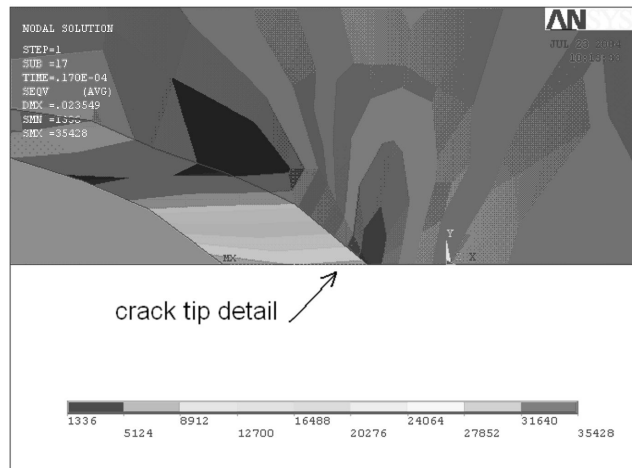


FIGURE 10. Finite Element Model for the cracked tubular section analyzed.



a)



b)

FIGURE 11. Von Mises Stress field: a) for the complete model after 1 μ sec of load application, and b) at the crack tip after 17 μ sec.

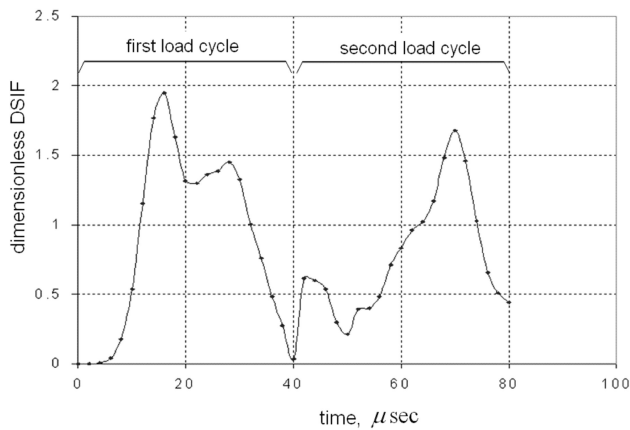


FIGURE 12. DSIF versus time for a centrally cracked tubular section.

solution [5], in which the cracked plate has infinite dimensions; thus, contributions of waves diffracted by the boundaries are nil.

The characteristic behavior of DSIF curves shown in Fig. 7 illustrates the strong influence of plate dimensions and crack size on the DSIF pattern.

In a second stage of the analysis, crack orientation has been varied in the model described above, which represents the problem assessed by Chen. Under these conditions, there is a mixed fracture mode when the stress waves reach the crack faces; in this study only mode I of the fracture has been considered in order to determine the DSIF. Orientation has been modeled by varying crack angles as follows: 0, 22.5, 45, 67.5, and 90°.

Figure 8 shows DSIF variation versus crack orientation. It can be seen that the DSIF for 0° is the case previously studied, where the crack faces are perpendicular to the stress wave. In the same figure, it can also be observed that, as the angle is increased, DSIF values decrease. For the case of a crack oriented at 90°, dilatational waves do not have any influence; thus, the DSIF value is nil. Moreover, for 90°, the effect of waves diffracted by the crack faces is negligible.

Figure 8 also shows that, for crack orientation 22.5°, DSIF values are close to those for the 0° case. Also, curve gradients for both cases are close, meaning that dilatational waves interact similarly. For orientations 45, 67.5 and 90°, the curve gradients are different and the DSIF is reduced, meaning that incident and reflected dilatational waves decrease in their interaction as the inclination is increased.

5. Analysis of a centrally cracked tubular section

In this section, results obtained from plates are compared with DSIF determined from a cracked tubular section. Tubular dimensions are: 12.2 cm long, 6.35 cm outside diameter and 0.32 cm wall thickness. Crack size is 2 cm in length, and material properties and applied load are the same as described in Sec. 2 and Fig. 1, respectively (see Fig. 9).

The mesh used consists of 1312 Solid95 elements of the ANSYS software. These elements have 20 nodes each; half

of the meshed model is shown in Fig. 10 due to symmetry simplifications. As previously explained, boundary conditions (were introduced into the model) to provide continuity for displacements and tractions horizontally and vertically. Mesh refinement at the crack tip can also be seen in Fig. 10. As in the plate model to simulate the singularity, 24 elements were used at the crack tip to determine the DSIF.

Figure 11a shows von Mises stress contours of the dilatational wave traveling towards the crack at time 1 μsec after the load was applied. Figure 11b shows stress concentrations at the crack tip at the time of the maximum DSIF value, which is at 17 μsec after the load was applied, as shown in Fig. 12.

From Fig. 12 it can be determined that the DSIF pattern shown for this particular tubular section is quite similar to that showed in the flat plate previously analyzed, thus indicating that the stress waves are interacting similarly in both cases. A generalized conclusion can only be obtained by comparing results from analyses with varying diameter and thickness, keeping crack and tubular section lengths constant in order to rule out curvature effects. It can be expected that edge effects are nil for the case of stress waves traveling parallel to the crack faces, since structural edges in tubular sections are nonexistent in this direction. Figure 12 shows two loading cycles where the second cycle which starts at 40 μsec, produces DSIF of less magnitude than those from the first cycle. This is due to the effect of a heavier influence of dilatational wave interaction. For a elapsed time after the load is applied that is much longer than shown in Fig. 12, wave diffractions vanish and the stress field would become stationary; thus, dimensionless DSIF values would tend to 1.

6. Conclusions

DSIF shows strong variations due to the effect of reflected and diffracted wave interactions with structural boundaries and crack geometry. On the other hand the solution given by B.R. Baker for a semi-infinite crack contained in an infinite and elastic medium shows a growing function, since there can be no effect from waves either reflected or diffracted by the nearby boundaries.

For the centrally cracked plates and tubular section analyzed, it has been observed that the effect of dilatational waves on DSIF values at the crack tip is dominant. Interaction of transversal and Rayleigh waves lower the maximum stresses reached during each of the dilatational loading cycles.

It has been preliminarily identified that, for centrally cracked plates and cracked tubular sections, DSIF variation due to wave interaction is similar in both cases and is mainly driven by load and unload cycles of dilatational or compression waves.

Acknowledgements

The authors would like to thank the Instituto Mexicano del Petróleo for the support given in producing this paper, and to the editor's reviewer for the valuable comments given to this work.

-
1. A.A. Griffith, *Philosophical Transactions of Royal Society of London* **A221** (1921) 163.
 2. E.H. Yoffe, *Philosophical Magazine* **42** (1951) 739.
 3. J.W. Craggs, *Journal of the Mechanics and Physics of Solids* **8** (1960) 66.
 4. K.B. Broberg, *Archiv. für Physik* **18** (1960) 159.
 5. B.R. Baker, *Journal of Applied Mechanics, Transactions ASME* **29** (1962) 449.
 6. G.C. Sih, *Journal of Fracture Mechanics* **4** (1968) 51.
 7. J.D. Achenbach and R. Nuismer, *International Journal of Fracture Mechanics* **7** (1971) 77.
 8. L.B. Freund, *Journal of Mechanics and Physics of Solids* **21** (1972) 47.
 9. Y.M. Chen, *Engineerig Fracture Mechanics* **7** (1975) 653.
 10. A. Frangi, Some Developments in the Symmetric Galerkin Boundary Element Method, Tesis Doctoral del Politecnico de Milano (1998).
 11. A. Rodríguez C., F.J. Sánchez Sesma, L.H. Hernández G., and G. Urriolagoitia C., *Científica ESIME-IPN* **21** (2000) 3.
 12. F. Chirino and J. Domínguez, *Engineering Fracture Mechanics* **34** (1989) 1051.
 13. K. Hellan, "Introduction to fracture mechanics" (McGraw-Hill Book Company, New York 1985).
 14. L.B. Freund, *Journal of the Mechanics and Physics of Solids* **21** 47.
 15. O.C. Zienkiewics, "The finite element method" (McGraw-Hill book company, London, UK, 1977).
 16. R.W. Clough and J. Penzien, "Dynamics of structures" (McGraw-Hill international editions, New York, USA, 1993).
 17. ANSYS, "Reference manual" (ANSYS Company, 1999).